Towards a low-noise axial fan for automotive applications

Towards a low-noise axial fan for automotive applications

Nicola Casari*, Stefano Oliani, Michele Pinelli, Mattia Piovan
University of Ferrara - Department of Engineering, Ferrara, Italy

Elisa de Paola, Luana G. Stoica, Alessandro Di Marco
Department of Engineering, University of Roma TRE, Rome, Italy

Enrico Mollica
SPAL Automotive Srl,Correggio RE, Italy

E-mail: *nicola.casari@unife.it

Abstract. The demand for quieter vehicles is pushing manufacturers of components for the automotive industry to seek for solutions to reduce the overall noise emissions. The cooling fan makes no exception: the aerodynamic interaction of the blades with the incoming flow generates turbulence and pressure fluctuations which ultimately translate into noise generation. A variety of expedients have been introduced to limit the produced noise, but no univocal solution has been found.

In modern research, Computational Fluid Dynamics (CFD) has been successfully applied to blades and fans for both the flow and acoustic field derivation. By including the acoustic field, researchers have been able to predict the effect of changes in the blade geometry on the overall sound emission. This work reports a conjugate numerical-experimental study of a reference profile in different flow conditions, in order to validate the CFD acoustic prediction and to lay the basis for improved candidates able to lower the fan-generated noise.

1. Introduction

Automotive fans, small wind turbines, and manned and unmanned aerial vehicles (MAVs/UAVs) are just a few of the examples in which noise generated by the flow interaction with the aerodynamic surfaces is a major concern. The always quieter vehicles (also considering the increasing share of electric cars) is pushing manufacturers to reduce the overall noise generated by the fan and other auxiliary units. Similarly, there is an interest in less noisy wind turbines: the increasing share of renewable energy in the worldwide electrical generation will require wind farms to be placed in proximity of human habitats. Lastly, UAVs (e.g. drones) often produce a significant amount of acoustic noise that interferes with their operation in urban and other inhabited areas, particularly during take-off, landing, and low-level flight. This is one of the aspects which are hindering the development of urban air mobility. For all of these applications, the flow regime in what is typically referred to as a low-to-moderate Reynolds number ($< 5e5$) is of great interest. In this regime, a limited number of tests and numerical data are available for the prediction of both aerodynamic performance and noise generation.

In light of these considerations, suppressing noise is a major goal that manufacturers are pursuing in order to comply with the standards (D.L. 277/1991, [1]), remove barriers to new technologies (EASA 2021) and reduce the possible hazard deriving from the usage of existing (but noisy) technologies [2]. Among the other areas, automotive noise has become a relevant focal point in the automotive industry, and a major contributor to the overall noise is the cooling fan. Consequently, the design process of automotive cooling fan systems cannot exclude their acoustic performances. Noise radiated by fans can be divided into two main components: the tonal component occurring at the blade passage frequency harmonics, and the broadband noise component. Several mechanisms concur to this latter component. The blade or fan self-noise component is the one generated by blades operating in a clean undisturbed flow [3], thus it represents the minimum noise a fan would emit, even when no installation effects are involved. Another contribution is represented by the noise due to the upstream turbulence ingested by the rotor, shed for instance by other parts of the automotive cooling module. An important mechanism involved is the trailing-edge noise, caused by the interaction of the blade turbulent boundary layer with the geometrical discontinuity represented by the Trailing Edge. In addition, blade tip vortices and leakage flows may also contribute significantly to fan noise [4].

The research in the aeroacoustic field is very active in two particular approaches: low-noise airfoil shapes and leading/trailing edge serrations. The first approach, for example, has led to the development of the CQU-DTU-LN series of airfoils with a reduction in noise generation of up to 5 dB with respect to a competitive NACA-6 digit airfoil ([5]). Parallelly, the introduction of a non-monotonic TE thanks to serrations has proven to be effective in reducing noise. The improvements have been confirmed both theoretically and experimentally showing a maximum noise reduction of about 10 dB ([6]). Still unclear remains the effect of leading-edge serrations on the overall self-noise generation: both improvements and deterioration of the overall sound pressure level (SPL) are detected depending on the angle of attack [7]. The study of the coupled aerodynamic and acoustic performance of turbomachinery blades has been historically carried out by means of analytical or semi-empirical approaches and experimentally. In addition, the inclusion of novel features for noise reduction has been driven by experience, even if supported by analytical and experimental analyses. More recently, great efforts are being made for the optimization of ducted fans in terms of aerodynamic performances, relying on CFD simulations. For instance, [8] and [9] use parametrized RANS and metamodels to mitigate the high computational cost of the complex numerical simulations and perform the optimization process using multi-objective genetic algorithms while [10] relies on RANS simulations and a Kriging metamodel, using Latin Hypercube Sampling to reduce the number of simulations required. Still few design optimization attempts have been made that include fan acoustic performances, such as [11], in which BEM and Ffowcs William-Hawkings analogy (FWH) [12] are used to compute the fan acoustics and a genetic algorithm performs the blades geometry optimization.

This work presents a combined experimental, semi-empirical (low-fidelity) and numerical (high-fidelity) analysis of a NACA 0012 airfoil. The aim of the authors is to show the various level of accuracy that can be obtained with the low- and high-fidelity tools. This comparison will represent the first step in a series of works which are devoted to the design of new low-noise profiles which are intended to replace the ones actually used for fan design.

2. Methodology

The availability of tools for the correct estimation of the self-noise generated by an airfoil in a flow is of crucial importance in order to design a silent airfoil. Moreover, it is likewise important to have different tools with various level of computational time required, as in the preliminary design phase, fast and lower-fidelity tools might be preferred over slower but higher-fidelity tools. Within this framework, two different computational packages are employed in this work:

what is referred to as Semi-empirical approach and Numerical Model. These are compared against the experiments in order to assess their accuracy. In the following, the experimental and computational tools are presented.

The reference case is a NACA 0012 profile with blunted TE. The TE thickness is 1 mm and the flow conditions are such that the chord-based Reynolds is 150,000 and the Angle of Attack is 5°. The chord length for the NACA generation is 50 mm.

2.1. Experimental set-up

Tests were performed at the Fluid Dynamics Laboratory in the Roma Tre University on a 3D printed NACA 0012 with a 50 mm chord and 200 mm span, at an angle of attack of 5° defined during the printing process. The airfoil was mounted on an aluminium stand, then fixed on an aluminium frame. A picture and a sketch of the set-up are shown in Figure 1. The reflections from the table where the frame was positioned were attenuated by means of a sound absorbing material, made of 100 mm high pyramidal elements. The measurement chain included a BSWA microphone, model MPA416, connected to a National Instruments BNC 2110 terminal block, and then acquired with a NI PXI-6143 DAQ using LabVIEW. The microphone was fixed on the frame, above the suction side of the airfoil, at a distance of about 5 times the chord, aligned with the trailing edge, in order to measure mainly the trailing edge noise.
The flow was provided by a subsonic jet with a circular nozzle of 50 mm diameter, located at a distance of 1.5 nozzle diameters from the airfoil, where it was verified that the velocity profile inside the jet is uniform. The airfoil was mounted horizontally, centered with respect to the jet nozzle, and was tested at 45 m/s, corresponding to a chord-based Reynolds of $1.5 \cdot 10^5$.

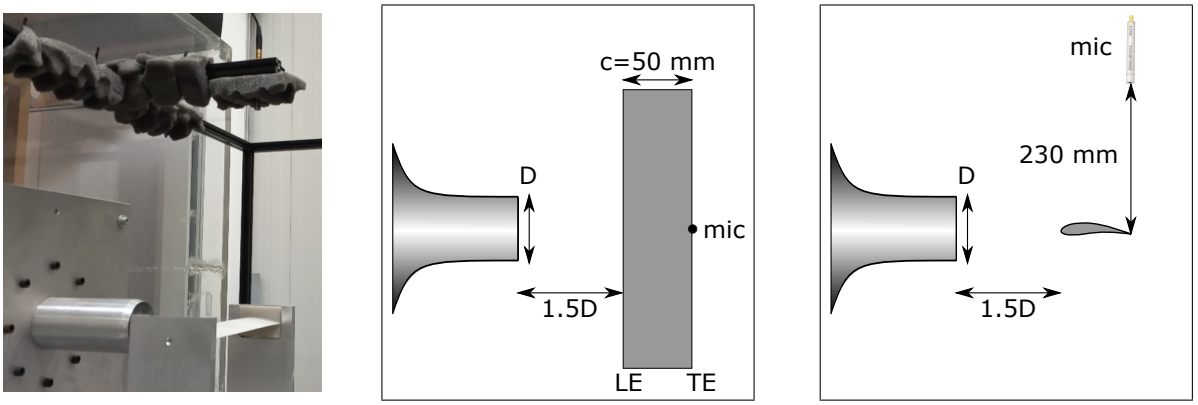

(a) (b) (c)

Figure 1: Experimental set-up for acoustic measurements: a) picture; b) upper view c) side view.

2.2. Semi-empirical approach

Brooks *et al* [13] have developed a semi-empirical model for the airfoil self-noise prediction. The authors developed a model (named here BPM after Brooks, Pope and Marcolini), by correlating the results of a series of aeroacoustic wind tunnel tests. Specifically, the authors have gathered a number of subsonic tests on different profiles and proposed a correlation of the noise generated by a generic profile based on the Reynolds number and on the angle of attack. Specifically, the authors divided the noise generated by the airfoil according to different elemental mechanisms:

- Turbulent-Boundary-Layer-Trailing-Edge (TBL-TE);

- Separation stall;
- Laminar-Boundary-Layer Vortex-Shedding (LBL VS);
- Tip vortex formation;
- Trailing-Edge-Bluntness Vortex-Shedding.

The model proposed by the authors in [13] is based on the scaling of the experimentally obtained noise spectra on a NACA 0012 profile with Reynolds numbers spanning from 4×10^5 to 1.5×10^6. The scaling law details are briefly reported here for future reference. Concerning the TBL-TE, the authors have taken inspiration from [14], leading to equation:

$$SPL_{TOT} = 10log_{10}(10^{SPL_p/10} + 10^{SPL_s/10} + 10^{SPL_\alpha/10}) \tag{1}$$

$$SPL_p = 10log_{10}\left(\frac{\delta_p^* M^5 L \bar{D}_H}{r^2}\right) + A\left(\frac{St_p}{St_1}\right) + (K_1 - 3) + \Delta K_1 \tag{2}$$

$$SPL_s = 10log_{10}\left(\frac{\delta_p^* M^5 L \bar{D}_H}{r^2}\right) + A\left(\frac{St_s}{St_1}\right) + (K_1 - 3) \tag{3}$$

$$SPL_\alpha = 10log_{10}\left(\frac{\delta_p^* M^5 L \bar{D}_l}{r^2}\right) + B\left(\frac{St_s}{St_2}\right) + K_2 \tag{4}$$

where the subscript p from Eqn. (2) and s from Eqn. (3) refer to the pressure and suction sides respectively, and SPL_α from Eqn. (4) is the angle dependent noise. This last term represents the additional noise due to boundary layer separation at high angle of attack. The overall noise level is found to scale with the displacement thickness δ^*, the Mach number M, the span L, the Strouhal number St the sound directivity $\bar{D}_h$ and $\bar{D}_l$ and the distance from the observer r. The scaling is obtained by introducing the spectral shape functions A and B and the amplitude functions K_1 and K_2.

With regards to LBL VS, the scaling law provided is:

$$SPL_{LBL-VS} = 10log_{10}\left(\frac{\delta_p^* M^5 L \bar{D}_H}{r^2}\right) + G_1\left(\frac{St'}{St'_{peak}}\right) G_2\left[\frac{Re_c}{(Re_c)_0}\right] + G_3(\alpha_*) \tag{5}$$

where the different spectral shape functions G_1, G_2 and G_3.

Brooks *et al* [13] also provided a correlation for the displacement thickness calculation, parameter which is crucial for the correct prediction of the generated noise. The correlation provided is valid for the NACA 0012 profile only and therefore could theoretically be applied here, assuming the TE truncation does not affect much the flow conditions on both the pressure and suction sides. However, with the perspective of extending the work to a number of profiles and for the sake of generality, a coupling with XFOIL [15] has been developed. In such a fashion a fully automatic procedure suitable for optimization processes is set-up, calling XFOIL for the calculation of the boundary layer parameters and implementing the BPM model for the noise prediction.

2.3. Numerical model

The high-fidelity setup has been obtained with the usage of the open source CFD package OpenFOAM-v2106. Specifically, a fully structured C-type grid has been realized on the truncate NACA 0012 profile, with a 3D development span equal to 1/3 of the chord. Cyclic boundary conditions have been imposed on the two lateral walls. The grid is composed of 8,320,000 hexahedrons, and in proximity of the wall the typical grid size for a Large Eddy Simulation

(LES) has been imposed - $x^+ = 50$, $y^+ = 1.5$ and $z^+ = 20$. The overall setup is reported in Fig. 2.

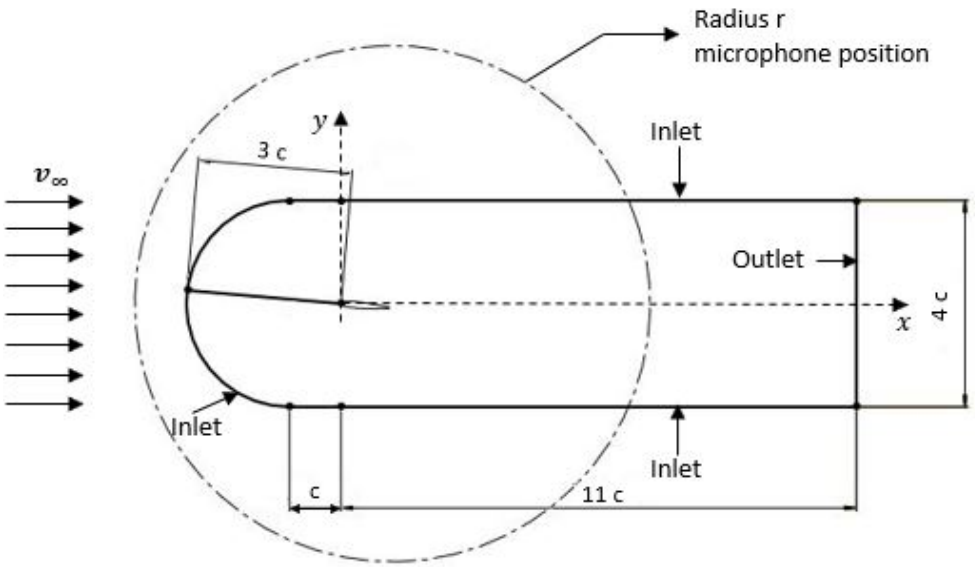

Figure 2: Representation of the numerical domain

In order to correctly capture the SPL a LES is required, as the broadband noise is generated by the turbulence (as largely described in section 2.2). In OpenFOAM, Large Eddy simulation with implicit filtering is available for the modeling of the higher frequency vortices. In this work, the Wall-adapting local eddy-viscosity (WALE) Sub-Grid Scale model from [16] has been used in order to return the correct wall asymptotic behavior for wall bounded flows. To initialize the calculation, a steady RANS solution obtained with a Langtry-Menter k-ω SST turbulence model was obtained [17]. The transient simulation was carried out at a fixed time-step of 0.1 μs, in order to maintain the maximum CFL around the value of 0.3.

The acoustic problem was solved by exploiting the acoustic analogy proposed by Ffowcs-Williams and Hawkings [12], and integrated in OpenFOAM via the libacoustics tools from [18]. The official release of OpenFOAM-v2106 provides an acoustic tool based on the Curle analogy. However, this is rather limiting as it does not allow to account for surfaces in motion. Therefore, this third-party library has been exploited, having in mind future applications with moving walls. In this case the integration surface where the load and thickness noise contributions are evaluated is placed on the airfoil. However, the library supports also the usage of permeable surfaces.

3. Results

3.1. Experimental Results

Data were acquired for 10 seconds at a sampling frequency of 65536 Hz. The signal to noise ratio of the data acquired on the airfoil with respect to the background noise and the jet were verified, giving values of 30.8 dB and 12.9 dB respectively, thus the signal is clearly identified. The narrowband acoustic spectra were processed by using the Welch method, with blocks of 65536 samples using a Hanning window, and 50% data overlap, thus providing a frequency resolution of 1 Hz. The A-weighted third octave band acoustic spectra were also computed. Results are shown in Fig. 3 and compared with the jet contribution.

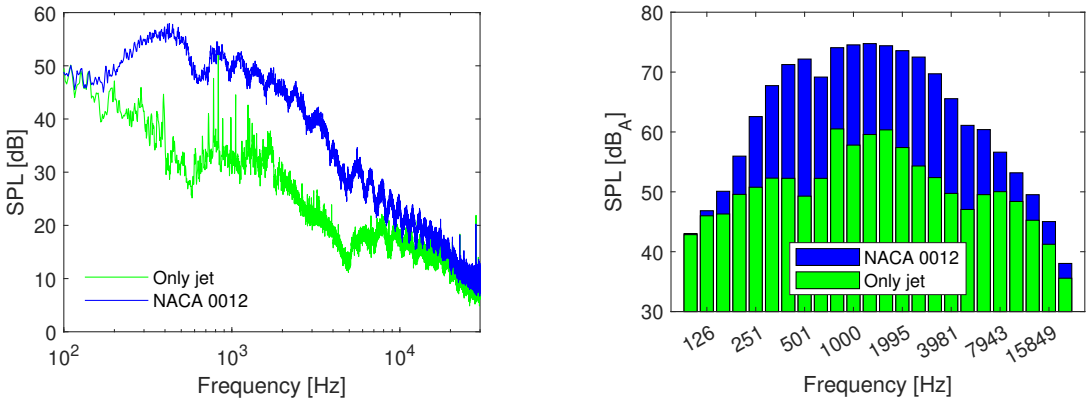

(a) (b)

Figure 3: Measured acoustic spectra: a) narrowband; b) A-weighted third octave band.

3.2. Semi-empirical Results

The results obtained by applying the BPM model are reported in Fig. 4. It can be clearly seen that the low-fidelity model is generally good in predicting the overall behaviour of the airfoil. Specifically, the most relevant features are captured, even if a 5-10 dB difference in the SPL and the distribution is displaced at slightly lower frequencies. The amplitude differences might be related to the absence of the background noise in the BPM case.

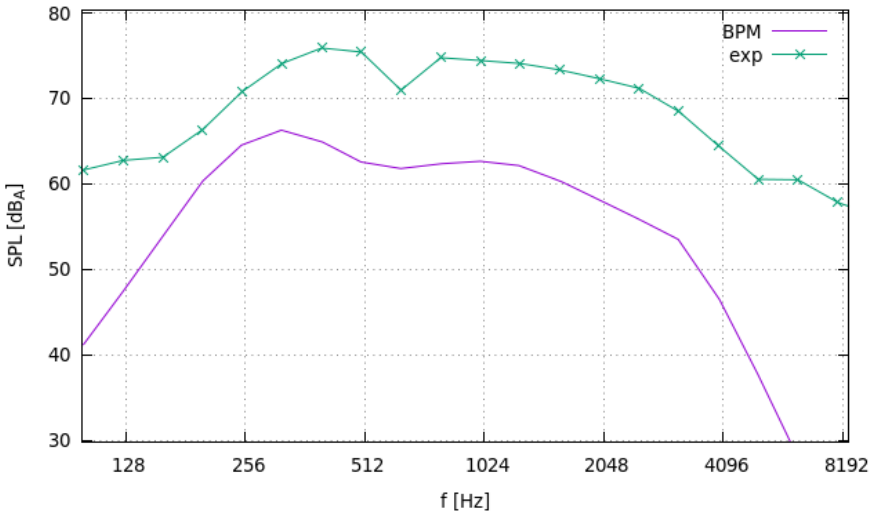

Figure 4: Comparison among experimental data and the BPM model in A-weighted third octave band

In particular, a shifted but consistent trend is well captured from 128 to 600 Hz. After the SPL peak at around 512 Hz, the experimental data show a dip which is rapidly recovered and a remarkably high SPL - above 70 dB$_A$ is maintained up to 2000 Hz. The semi-empirical model correctly replicate such behavior. At very high frequencies, the mismatch between experiments and the prediction increases. The reason behind this discrepancy is very likely related to the larger jet noise contribution, as clearly visible in Fig. 3.

It is now of interest to understand how the different noise sources contribute in the definition

of the overall SPL distribution. Figure 5 reports the overall SPL predicted by BPM and all the elemental components.

At the lowest frequencies, the Turbulent Boundary Layer contributions are the most relevant ones. In particular, the suction side BL is responsible for the lowest frequency noise. The peak at 256 Hz is due to the angle of attack, which causes separation on the suction side. The separation noise is therefore the highest noise source. The dip at 600 Hz is smoothed by the semi empirical approach and this is the results of the TBL-SS noise which remains high for frequencies up to 1000 Hz. The TE bluntness and the laminar boundary layer are the responsible for the noise production at higher frequencies. It is interesting to note that the small bluntness of the TE and originates the plateau which is identified also in the experimental data. Specifically, the 1 mm trailing edge bluntness applied (to reproduce the real component) has only a minor impact according to the BPM model. Similarly, the laminar BL produce a negligible noise if compared to the other sources.

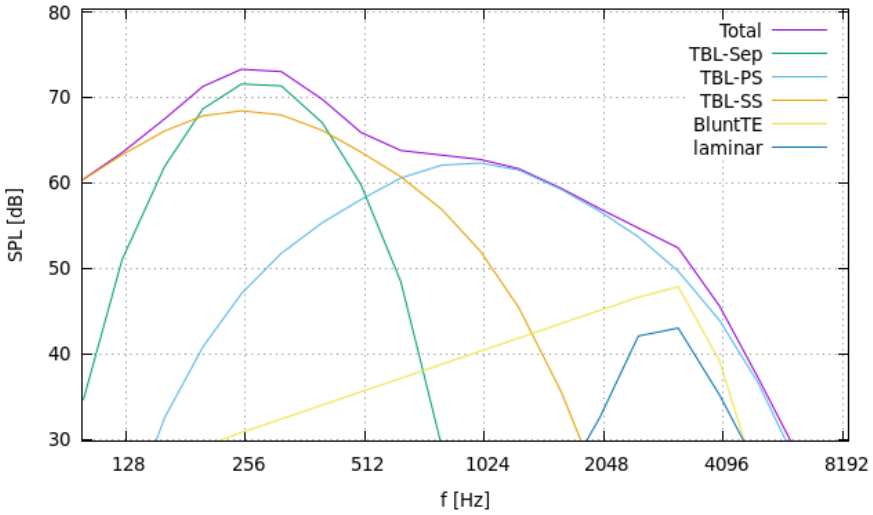

Figure 5: Noise source contributions to the overall SPL with the BPM model

3.3. Numerical Results

Under the conditions reported in section 2, the wind tunnel experimental performance are reported by Pope [19], giving a $C_L = 0.59$ and a $C_D = 0.0157$. The presence of a separation bubble makes the result unsteady and therefore the time averaged performance have been evaluated leading to a $C_L = 0.585$ and $C_D = 0.0164$. Therefore, a good agreement between the numerical results and the experimental data has been found, with a mismatch lower than 5%.

The acoustics results were obtained with the Ffowcs-Williams Hawkings analogy, in particular, the GT formulation (developed for a situation where both observer and profile remain fixed and the fluid has a velocity) was used. In fact, it is the typical setup of a wind tunnel with noise revelation equipment. The simulation covers 0.02 s of physical time and the acoustic measures (i.e. pressure perturbations) where sampled at each time step - corresponding to 0.5×10^{-6} s giving a CFL number around 0.4. The prediction of the noise generated applying such an analogy is shown in Fig. 6. In order to reproduce the SPL of the real profile, the same span should be considered. For this purpose, the correlation, taken from [20] and reported in (6) has been used

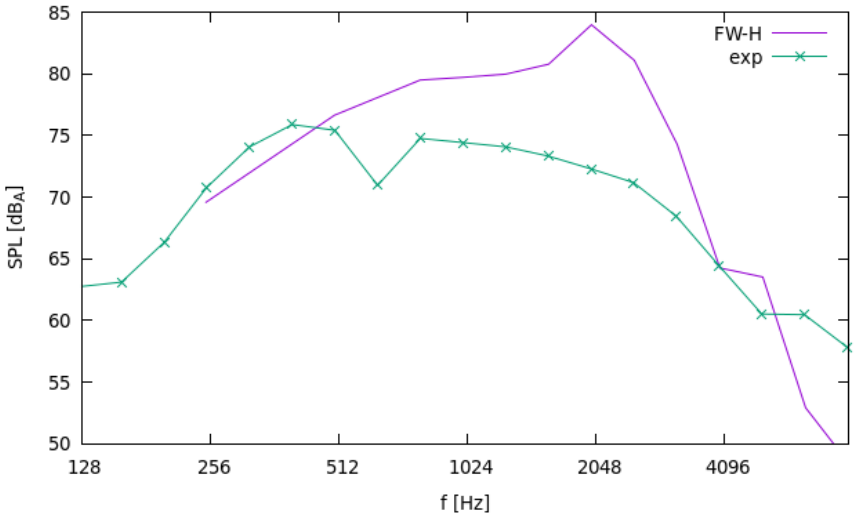

Figure 6: One-third octave band spectrum according to FW-H analogy

$$SPL_{eff} = SPL_{sim} + 10log_{10}\left[\frac{tan^{-1}(\frac{S_0}{r_{e,0}}) + \frac{sin\left(2\ tan^{-1}(\frac{S_0}{r_{e,0}})\right)}{2}}{tan^{-1}(\frac{S_1}{r_{e,0}}) + \frac{sin\left(2\ tan^{-1}(\frac{S_1}{r_{e,0}})\right)}{2}}\right] \tag{6}$$

where S_0 is the simulated span, S_1 is the real span of the airfoil wetted by the jet and $r_{e,0}$ is the position of the microphone from the origin of the coordinate system.

It can be clearly seen how the low frequency contributions are well captured. However, by reducing the wavelength, the FW-H analogy deflects from the experiments and tends to overestimate the noise contributions. At the highest frequencies of interest, the behaviour is reasonably well predicted, including the plateau around 4100 Hz.

The reason behind the mismatch between numerical and experimental data should not be related to an under-resolved wavelength spectrum in the LES. Indeed, the deflection occurs at the frequencies where according to the BPM model the contributions of the laminar vortex shedding and of the blunt TE become relevant. An analysis of the simulation metrics shows a Celik index between 0.83 and 0.95 in the entire domain, suggesting a good grid resolution. The authors believe that the overprediction of laminar contribution might be related to a underestimate of the incoming turbulence level, which is provided as boundary condition. Further computational investigations are being carried out in order to improve the predictions in this area.

4. Conclusions

In this work, a aeroacoustic investigation of a NACA 0012 profile with blunted trailing edge has been performed. The results shown here has been obtained by means of experiments and numerical tools. Specifically, an ad-hoc test bench has been developed for the description of the acoustic behaviour of the profile. A low-order semi-empirical method has been implemented for assessing its accuracy in the prediction of the SPL distribution. Eventually a full 3D-CFD LES has been carried out for an high-fidelity simulation of the aeroacoustic performance.

The BPM implementation, modified with data from xfoil, shows good agreement with the experiments, even though the overall distribution seems to be displaced at low frequency and slightly lower SPL. This assessment proves it is suitable for optimization procedures, given the low computational costs needed for obtaining such prediction. Concerning the LES simulation,

there is an unexpected mismatch with respect to the experiments and the reason might be related to a low-inflow turbulence. Further work will be devoted to the high-fidelity analysis of the profile.

References

[1] Doyle S, Scata D and Hileman J 2021 *INTER-NOISE and NOISE-CON Congress and Conference Proceedings* vol 263 (Institute of Noise Control Engineering) pp 5815–5827
[2] Nissenbaum M A, Aramini J J, Hanning C D *et al.* 2012 *Noise and Health* **14** 237
[3] Wright S 1976 *Journal of Sound and Vibration* **45** 165–223
[4] Moreau S and Roger M 2007 *AIAA journal* **45** 48–57
[5] Shen W Z, Zhu W J, Fischer A, García N R, Cheng J, Chen J and Madsen J 2014 *Journal of Physics: Conference Series* vol 555 (IOP Publishing) p 012093
[6] Moreau D J and Doolan C J 2013 *AIAA journal* **51** 2513–2522
[7] Lacagnina G, Chaitanya P, Kim J H, Berk T, Joseph P, Choi K S, Ganapathisubramani B, Hasheminejad S M, Chong T P, Stalnov O *et al.* 2021 *International Journal of Aeroacoustics* **20** 130–156
[8] Grondin G, Kelner V, Ferrand P and Moreau S 2005 *Proc. of the International Congress on Fluid Dynamics Applications in Ground Transportation, Lyon, France*
[9] Buisson M, Ferrand P, Soulat L, Aubert S, Moreau S, Rambeau C and Henner M 2013 *Computers & Fluids* **80** 207–213
[10] Henner M, Demory B, Gonon T and Helbert C 2019 *European Conference on Turbomachinery Fluid Dynamics and Thermodynamics*
[11] Zhong Y, Li Y, Li P, Chen J, Xia T and Kuang X 2021 *Journal of Physics: Conference Series* vol 1952 (IOP Publishing) p 032022
[12] Ffowcs Williams J E and Hawkings D L 1969 *Philosophical Transactions of the Royal Society of London. Series A, Mathematical and Physical Sciences* **264** 321–342
[13] Brooks T F, Pope D S and Marcolini M A 1989 Airfoil self-noise and prediction128 Tech. rep.
[14] Williams J F and Hall L 1970 *Journal of fluid mechanics* **40** 657–670
[15] Drela M 1989 *Low Reynolds number aerodynamics* (Springer) pp 1–12
[16] Nicoud F and Ducros F 1999 *Flow, turbulence and Combustion* **62** 183–200
[17] Langtry R B and Menter F R 2009 *AIAA journal* **47** 2894–2906
[18] Epikhin A, Evdokimov I, Kraposhin M, Kalugin M and Strijhak S 2015 *Procedia Computer Science* **66** 150–157
[19] A P 1954 *Wind Tunnel Testing* (John Wiley & Sons)
[20] Abdessemed C, Bouferrouk A and Yao Y 2021 *Acoustics* vol 3 (Multidisciplinary Digital Publishing Institute) pp 177–199